Journal of Physical and Chemical Reference Data

RESEARCH ARTICLE | AUGUST 28 2024

Ideal Gas Thermodynamic Functions For NO From the Total Partition Sum and Its Moments

Robert R. Gamache ; Nicholas G. Orphanos ; Qianwei Qu; Sergei N. Yurchenko ; Jonathan Tennyson

J. Phys. Chem. Ref. Data 53, 033103 (2024)
https://doi.org/10.1063/5.0209834

Journal of Physical and Chemical Reference Data ARTICLE pubs.aip.org/aip/jpr

Ideal Gas Thermodynamic Functions For NO From the Total Partition Sum and Its Moments

Cite as: J. Phys. Chem. Ref. Data 53, 033103 (2024); doi: 10.1063/5.0209834
Submitted: 23 March 2024 • Accepted: 16 July 2024 •
Published Online: 28 August 2024

Robert R. Gamache,[1,a)] Nicholas G. Orphanos,[1] Qianwei Qu,[2] Sergei N. Yurchenko,[3] and Jonathan Tennyson[3]

AFFILIATIONS

[1] Department of Environmental, Earth, and Atmospheric Sciences, University of Massachusetts Lowell, Lowell, Massachusetts 01854, USA
[2] Paul Scherrer Institut, 5232 Villigen, Switzerland
[3] Department of Physics and Astronomy, University College London, London WC1E 6BT, United Kingdom

[a)] **Author to whom correspondence should be addressed:** Robert_Gamache@uml.edu

ABSTRACT

The total internal partition sum, $Q_{int}(T)$, and the translational partition sum, $Q_{trans}(T)$, were computed for six isotopologues of NO: $^{14}N^{16}O$, $^{15}N^{16}O$, $^{14}N^{18}O$, $^{14}N^{17}O$, $^{15}N^{18}O$, $^{15}N^{17}O$. These were used to determine the total partition sum, $Q(T)$, and its first and second moments, $\tilde{Q}'(T)$ and $\tilde{Q}''(T)$. The total internal partition sum was computed using term values determined by Qu *et al.* [Mon. Not. R. Astron. Soc. **504**, 5768–5777 (2021)] for $^{14}N^{16}O$ and those of Wong *et al.* [Mon. Not. R. Astron. Soc. **470**, 882–897, (2017)] for the other isotopologues. These term values are the best available and hence provide the most accurate total internal partition sums and its first and second moments. The uncertainties in $Q_{int}(T)$, its moments, and the resulting thermodynamic functions were determined from the uncertainty in the term values and the uncertainty due to the convergence of the partition sum and its moments. From these quantities, the isobaric heat capacity, Helmholtz energy, entropy, enthalpy, Gibbs function, and the JANAF functions *hef* and *gef*, and their uncertainties, were computed on a 1 K grid from 1 to 9000 K. The data are compared with the literature values. The resulting thermodynamic quantities are the most accurate determined from direct summation of $Q(T)$, $\tilde{Q}'(T)$, and $\tilde{Q}''(T)$.

Published by AIP Publishing on behalf of the National Institute of Standards and Technology. https://doi.org/10.1063/5.0209834

CONTENTS

List of Tables

List of Figures

1. Introduction

Nitric oxide (chemical formula NO) is present throughout the universe. In 1990, the first detection of interstellar NO in the cold dark cloud L134N was done by McGongle *et al.*[2] Several years later, Gerin *et al.*[3] detected two rotational transitions of nitric oxide in six molecular clouds: at two oppositions in the dark cloud L134N and in five giant clouds, OMC1, W51, SgrB2, SgrA + 20 km/s and +50 km/s clouds. Then Gerin *et al.*[4] reported the abundance of NO in the dark cloud TMC 1. In several works, Martín *et al.*[5–7] reported the first detections of SO_2, NS, and NO in an extragalactic source, the nucleus of the starburst galaxy NGC 253. In 2007, Akyilmaz *et al.*[8] measured two NO transitions in the pre-protostellar cores L1544 and L183. In 2013, Quintana-Lacaci *et al.*[9] detected the emission of circumstellar nitric oxide for the first time in one of the most massive and luminous stars, IRC +10420. While not yet detected in exoplanet atmospheres, NO is a potential biomarker. In recent work for the 2025 launch of the Spektr-UF (WSO-UV) space observatory, Tsurikov and Bisikalo[10] estimated the possibility of detecting the transmission of light in the NO γ-bands in the atmospheres of exoplanets.

The δ and γ bands of NO are responsible for nightglow on Earth, Venus, and Mars. Eastes *et al.*[11] measured the nightglow from Earth using the S3-4 satellite. In 2008, Gérard *et al.*[12] observed the NO nightglow on Venus using SPICAV on board Venus Express and Cox *et al.*[13] made observations of the nightglow with the SPICAM ultraviolet spectrometer on board the Mars Express orbiter. Nitric oxide is an important molecule in the Earth's atmosphere. HITRAN[14] lists NO as molecule #8 for absorbing infrared radiation in the atmosphere. In the troposphere, NO is mainly produced by anthropogenic sources such as combustion[15] and soil cultivation and along with N_2O catalyzes the production of tropospheric ozone. In the stratosphere, NO originates from the reaction of N_2O with $O(^1D)$ and is a proxy for ozone depletion.[16,17] NO and other nitrogen oxides are important compounds in air pollution, rocket propulsion, and chemical industries. These species are used to process semiconductors and play important roles in medical and environmental sciences. As such, there is a need to have accurate thermodynamic quantities for NO.

In this work, the thermodynamic functions were calculated for the six isotopologues of NO: $^{14}N^{16}O$, $^{15}N^{16}O$, $^{14}N^{18}O$, $^{14}N^{17}O$, $^{15}N^{18}O$, and $^{15}N^{17}O$. The thermodynamic functions were determined from the total internal partition sum (TIPS) and its first two moments over the temperature range 1–9000 K. The convergence of the partition sum and its moments was studied to ensure convergence of all quantities and an uncertainty analysis of the thermodynamic functions is given as a function of temperature.

2. The Total Partition Sum and Its Moments

The total partition sum is given by the product of the TIPS (described in Sec. 2.1) times the translational partition sum

$$Q_{total}(T) = Q_{int}(T)Q_{trans}(T). \quad (1)$$

The total internal molecular partition sum, $Q_{int}(T)$, is used to determine how molecules in thermodynamic equilibrium are distributed among the various energy states at a given temperature. An accurate knowledge of the TIPS is required for many applications, e.g., calculation of thermodynamic properties, evaluation of line intensities from spectra, correction of line intensities to temperatures other than those given in standard databases,[14,18] and the determination of relative abundances of different molecules in stellar atmospheres.[19]

The translational partition sum can be written in terms of the de Broglie wavelength, $\Lambda = h/(2\pi\, m\, k\, T)^{1/2}$, and the molar volume of the system, V/n,

$$Q_{trans}(T) = \frac{\overline{V}}{\Lambda^3} = \frac{kT}{p\Lambda^3}, \quad (2)$$

where h is Planck's constant, m is the mass of the molecule, k is Boltzmann's constant, T is the temperature in kelvins. The second expression for Q_{trans} in Eq. (2) is from applying the *ideal gas* equation, $pV = nkT$. All fundamental physical constants are taken from 2018 CODATA.[20]

2.1. Total internal partition sum

The TIPS[21–23] is given by

$$Q(T) = \sum_{\text{all states}\ i} g_i \exp\left(-\frac{hcF_i}{kT}\right), \quad (3)$$

Published by AIP Publishing on behalf of the National Institute of Standards and Technology

where g_i and F_i are the degeneracy and term value of the state i, c is the speed of light, and the other factors were defined above. The term values are in cm^{-1} units. The zero of energy for NO is the $J = 0.5$ state of the ground vibrational state and ground electronic state, $X^2\Pi$. The degeneracy term, g_i, is composed of several parts. First are degeneracies associated with the molecule[24] and are state-independent. Examples are degeneracies due to the spin of nuclei not involved in symmetry operations [see Eq. (1) of Ref. 25 for the d_i factor]. This degeneracy factor is expressed as $\Pi(2I + 1)$, where I is the nuclear spin of the nuclei not interchanged by rotation and the product is taken over all nuclei not interchanged by rotation. The nuclear spins I of ^{14}N and ^{15}N are 1 and 1/2, respectively, while the nuclear spins I of ^{16}O and ^{18}O are both 0. Thus, the state-independent spin factors are 3, 3, 2 for the $^{14}N^{16}O$, $^{14}N^{18}O$, $^{15}N^{16}O$ isotopologues, respectively. However, for NO it is more complicated. NO is an open-shell molecule and some energy formulas include these spin factors, e.g., for $^{14}N^{16}O$ some formulations give for each J value 3 states, $F = J \pm 1$, 0, and other formulations only include 2 of the F states, in which case Q is multiplied by 1.5 to get the correct value. Note that the quantum number F is different than the label for term values, F_i. These factors are discussed more below. The second are degeneracies due to the symmetric interchange of like atoms[21,26] [the d_s term in Eq. (1) of Ref. 25], which is not applicable here due to the symmetry of NO. Last are the degeneracies of the rotational states that are given $2F + 1$ or $2J + 1$, depending on whether the hyperfine structure is resolved or not.

The electronic ground state of the NO molecule is a $X^2\Pi$ state that is split by spin-orbit interaction giving the $^2\Pi_{1/2}$ state and $^2\Pi_{3/2}$ state, which are separated by about 123 cm^{-1}. The interaction with electronic states of Σ symmetry causes each of these two states to be split by Λ-doubling into doublets with components split by 10^{-2} to 10^{-3} cm^{-1}. Using the molecular constants of Meerts[27] for $^{14}N^{16}O$ and those of Amiot *et al.*[28] for the $^{15}N^{16}O$ and $^{14}N^{18}O$ isotopologues, Gamache *et al.*[25] calculated the term values for these isotopologues of NO and determined the TIPS using the product approximation [$Q_{int}(T) = Q_{vib}(T)\, Q_{rot}(T)$] because at that time data on other vibrational and electronic states was limited. The term values obtained from the constants of Meerts and Amiot *et al.* consider the hyperfine splitting of states, i.e., labeled by J, F, and e or f. Since that time, *ab initio* calculations have become available. Wong *et al.*[29] calculated the term values for the electronic ground state of the $^{14}N^{16}O$, $^{14}N^{18}O$, $^{15}N^{16}O$, $^{14}N^{17}O$, $^{15}N^{18}O$, and $^{15}N^{17}O$ isotopologues. The calculations considered from the ground vibrational state to $v_{max} = 51$ and yield term values to ~52 000 cm^{-1}. Later, Qu *et al.*[30] extended the *ab initio* calculations to include rovibronic states of $^{14}N^{16}O$ corresponding to the γ, β, and δ band systems along with minor improvements for states in the $X^2\Pi$ ground state. Note that these states do not consider the hyperfine interaction.

In this work, the TIPS was computed using the term values of Qu *et al.*[30] for the rovibronic $X^2\Pi$, $A^2\Sigma^+$, $B^2\Pi$, and $C^2\Pi$ states of $^{14}N^{16}O$ and those of Wong *et al.*[29] for the rovibronic $X^2\Pi$ states of $^{15}N^{16}O$ and $^{14}N^{18}O$. TIPS were computed for the 3 lesser isotopologues, $^{14}N^{17}O$, $^{15}N^{18}O$, and $^{15}N^{17}O$, using the term values of Wong *et al.* to allow the determination of the thermodynamic quantities for a natural sample. They are not presented here but can be obtained upon request to the corresponding author or from zenodo (https://doi.org/10.5281/zenodo.12635229).

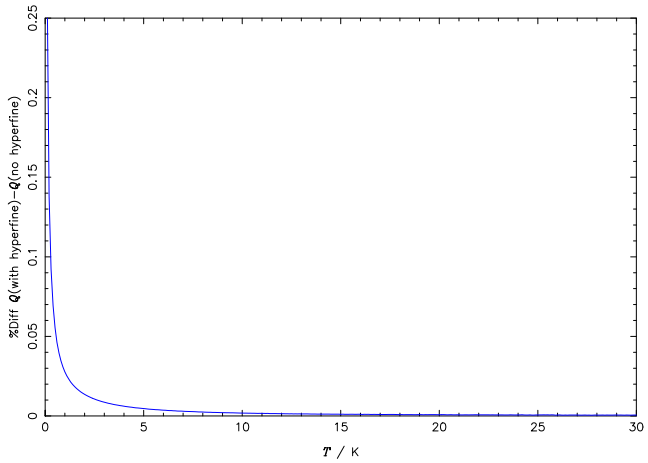

FIG. 1. The percent difference (PD) in $Q_{int}(T)$ calculated using term values determined including the hyperfine terms and term values that do not (no hyperfine terms) versus temperature.

In order to determine the TIPS, one needs the energy eigenvalues or term values for the molecule/isotopologue in question. Here, the six isotopologues of NO are considered. The calculations of the TIPS used the term values of Qu *et al.*[30] for the rovibronic $X^2\Pi$, $A^2\Sigma^+$, $B^2\Pi$, and $C^2\Pi$ states of $^{14}N^{16}O$ and Wong *et al.*[29] for the ground electronic states of $^{15}N^{16}O$, $^{14}N^{18}O$, $^{14}N^{17}O$, $^{15}N^{18}O$, and $^{15}N^{17}O$. Because the hyperfine interaction was not considered in the *ab initio* calculations, tests were made to consider the effect of the splitting on $Q_{int}(T)$. Calculations were made for $^{14}N^{16}O$ using the term values determined using the molecular constants of Meerts[27] (hyperfine terms included) and those of Wong *et al.*[29] The term values from the formulation of Meerts are only for the ground vibrational state, but these are sufficient for calculating Q_{int} at low temperatures. Figure 1 shows the percent difference (PD) in Q_{int} calculated using the term values with the hyperfine interaction terms (Meerts' formulation) minus that from using the Wong *et al.*[29] term values versus temperature. The difference between the two calculations is ~0.25% at 1 K and reaches zero by 25 K. Thus in the calculations below the term values of Wong *et al.*[29] are used. Note that Wong *et al.*[29] computed $Q_{int}(T)$ in their work using physical constants from the NIST website from 2012, whereas in this work the 2018 CODATA[20] constants were used. There are very small differences in the constants. Thus, the $Q_{int}(T)$ computed here have small differences beginning in the seventh significant digit compared with the work of Wong *et al.*

Looking at Eq. (3), at a given temperature, there will be a point where the term values are so large the exponential will no longer contribute to the partition sum. At this point the TIPS is considered converged. Where this happens in energy space is quite difficult to determine and different methods have been used. Gamache *et al.*[22] used a criterion of comparing the partition sum evaluated over sorted energies at 3/4 of the energies versus all the energies. This method works if the energy levels being used are complete and the percent error between the two methods is less than a preset criterion for a given temperature. Furtenbacher *et al.*[31] estimated the uncertainty in the convergence of Q_{int} by calculating a term they labeled

$Q^{missing}$, which is an contribution to Q_{int} for states that are above the last energy in the data set used to determine Q_{int}. This method is difficult to apply as it requires the density of states and average J to be estimated and it will have an associated uncertainty, which is large. In a study on N_2, Gamache and Orphanos[32] considered the effects on convergence of summing to different J_{max} values and comparing the resulting Q_{int} values as a function of temperature.

2.2. First and second moments of the partition sums

The thermodynamic functions can be determined in terms of the total partition sum and its derivatives or its first and second moments.[23,33,34] The expressions using the moments are more concise and are used below. The first moment of the TIPS is

$$\tilde{Q}'_{int}(T) = T\frac{dQ_{int}(T)}{dT} = \sum_{\text{all states } i} g_i\left(\frac{hcF_i}{kT}\right)\exp\left(-\frac{hcF_i}{kT}\right) \quad (4)$$

and the second moment is

$$\tilde{Q}''_{int}(T) = T^2\frac{d^2Q_{int}(T)}{dT^2} + 2\tilde{Q}'_{int}(T) = \sum_{\text{all states } i} g_i\left(\frac{hcF_i}{kT}\right)^2\exp\left(-\frac{hcF_i}{kT}\right). \quad (5)$$

The first and second moments of the translational partition sum[34] are

$$\tilde{Q}'_{trans}(T) = T\frac{dQ_{trans}(T)}{dT} = \frac{5}{2}\frac{kT}{p\Lambda^3} \quad (6)$$

and

$$\tilde{Q}''_{trans}(T) = T^2\frac{d^2Q_{trans}(T)}{dT^2} + 2\tilde{Q}'_{trans}(T) = \frac{35}{4}\frac{kT}{p\Lambda^3}. \quad (7)$$

Using these expressions, the first and second moment of the total partition sum are

$$\tilde{Q}'(T) = \tilde{Q}'_{int}(T)Q_{trans}(T) + Q_{int}(T)\tilde{Q}'_{trans}(T) \quad (8)$$

and

$$\tilde{Q}''(T) = \tilde{Q}'_{int}(T)Q_{trans}(T) + Q_{int}(T)\tilde{Q}''_{trans}(T) + 2\tilde{Q}'_{int}(T)\tilde{Q}'_{trans}(T). \quad (9)$$

2.3. Evaluation of $Q_{int}(T)$, $\tilde{Q}'_{int}(T)$, and $\tilde{Q}''_{int}(T)$ and their uncertainties

To evaluate the partition sum and its moments, the term values from Qu *et al.*[30] and Wong *et al.*[29] were used. The term values for the $X^2\Pi$, $A^2\Sigma^+$, $B^2\Pi$, and $C^2\Pi$ states of $^{14}N^{16}O$ are complete to ~62 000 cm^{-1}, well above the dissociation limit of ~52 400 cm^{-1},[29,35] and those of the $X^2\Pi$ electronic states of $^{15}N^{16}O$, $^{14}N^{18}O$, $^{14}N^{17}O$, $^{15}N^{18}O$, and $^{15}N^{17}O$ are complete to ~52 000 cm^{-1}. The calculations of $Q_{int}(T)$ were made for each isotopologue and with cut-offs in J at 145.5, 155.5, 165.5, 174.5, and 184.5. The PD between these values of the internal partition function were determined, which provide an estimate of the convergence of the partition sums as a function of temperature.

Figure 2 shows the PD in TIPS for $^{14}N^{16}O$ computed by summing to different J_{max} values. Plotted are the PDs versus temperature; the black line is the PD between $Q_{int}(J_{max} = 155.5)$ and $Q_{int}(J_{max} = 145.5)$, the red line is that for $Q_{int}(J_{max} = 165.5)$ and $Q_{int}(J_{max} = 155.5)$, the green line is that for $Q_{int}(J_{max} = 174.5)$ and $Q_{int}(J_{max} = 165.5)$, and the blue line is the PD for $Q_{int}(J_{max} = 184.5)$ and $Q_{int}(J_{max} = 174.5)$. The plot suggests that $Q_{int}(J_{max} = 184.5)$ is converged to better than 0.016% at 9000 K, which is reasonable as the term values go ~10 000 cm^{-1} above the dissociation energy. At lower temperatures, the convergence is much better.

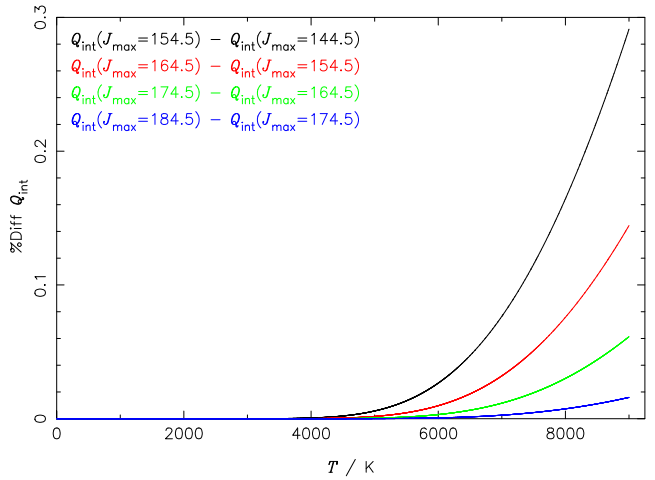

FIG. 2. The percent difference (PD) in $Q_{int}(T)$ for $^{14}N^{16}O$ computed by summing to different J_{max} values. Plotted are the PDs versus temperature; the black line is the PD between $Q_{int}(J_{max} = 154.5)$ and $Q_{int}(J_{max} = 144.5)$, the red line is that for $Q_{int}(J_{max} = 164.5)$ and $Q_{int}(J_{max} = 154.5)$, the green line is that for $Q_{int}(J_{max} = 174.5)$ and $Q_{int}(J_{max} = 164.5)$, and the blue line is the PD for $Q_{int}(J_{max} = 184.5)$ and $Q_{int}(J_{max} = 174.5)$.

Similar figures for the first and second moments of the partition sum, $\tilde{Q}'_{int}(T)$ and $\tilde{Q}''_{int}(T)$ for $^{14}N^{16}O$ are available in the supplementary material. The $\tilde{Q}'_{int}(T)$ and $\tilde{Q}''_{int}(T)$ are converged to better than 0.064% and 0.163%, respectively, at 9000 K (see Figs. 1S and 2S).

Another component to the uncertainty in Q_{int} and its moments are the uncertainties in the term values reported by Qu *et al.*[30] and by Wong *et al.*[29] Their uncertainty analysis is based on the source of the data. When the term values were determined in the MARVEL analysis,[30,36] the MARVEL uncertainties were used. MARVEL works by setting up of a vector containing all the experimentally measured transitions selected [called a Spectroscopic Network (SN)], another one comprising the requested MARVEL energy levels, and a matrix which describes the relation between the transitions and the energy levels. In the solution of the set of linear equations, uncertainties in the measured transitions are incorporated which result in uncertainties of the energy levels determined. Interested readers should see Refs. 36 and 37. Uncertainties for the other states are estimated by comparing the *ab initio* calculations for the particular electronic states to measurement and extrapolating where no measurements are available (see Figs. 6 and 7 of Ref. 30 for details). While the information available does not allow a rigorous statistical meaning to the uncertainties they present, it is reasonable and conservative to consider them as standard uncertainties. Using these uncertainties, the TIPS and its moments were recalculated using the term value plus

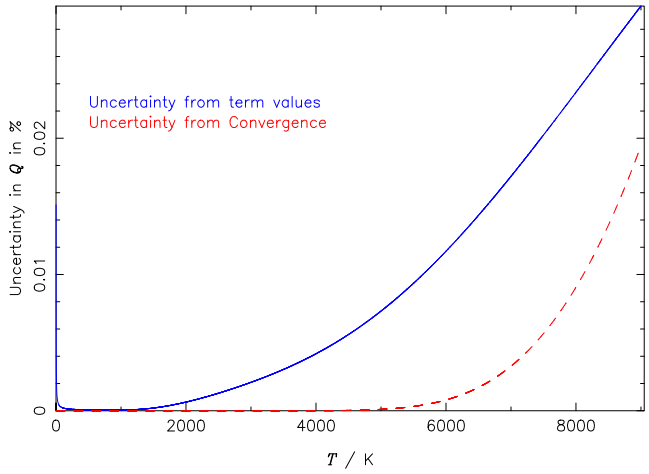

FIG. 3. The relative uncertainty in $Q_{\text{int}}(T)$ from the uncertainty from convergence (red dashed line) and from the uncertainty in the term values (blue solid line) versus temperature.

the uncertainty. These functions were compared to those calculated above from the term values to determine the uncertainty as a function of temperature. In Fig. 3, the uncertainty from convergence (red dashed line) and from the uncertainty in the term values (blue solid line) for $Q_{\text{int}}(T)$ are plotted versus temperature. The uncertainty in $Q_{\text{int}}(T)$ from the term values is always larger than the convergence uncertainty but is still less than 0.03%. Figures for $\tilde{Q}'_{\text{int}}(T)$ and $\tilde{Q}''_{\text{int}}(T)$ are included in the supplementary material (Figs. 3S and 4S). For both moments, the convergence uncertainty dominates.

3. Evaluation of the Thermodynamic Quantities

Given the functions $Q(T)$, $\tilde{Q}'(T)$, and $\tilde{Q}''(T)$, $Q_{\text{int}}(T)$, $\tilde{Q}'_{\text{int}}(T)$, $\tilde{Q}''_{\text{int}}(T)$, $Q_{\text{trans}}(T)$, $\tilde{Q}'_{\text{trans}}(T)$, and $\tilde{Q}''_{\text{trans}}$, the ideal gas thermodynamic functions can be determined for each isotopologue. A complete derivation of all thermodynamic quantities using derivatives and using the moments can be found at zenodo (https://doi.org/10.5281/zenodo.12635229). Below, the equations using the moments of the partition sum are used. The relationships among the thermodynamic quantities have been checked for consistency. The Helmholtz energy is given by

$$A(T) = -RT \ln Q(T) \tag{10a}$$

$$A(T) = -RT \ln Q_{\text{int}}(T) - RT \ln Q_{\text{trans}}, \tag{10b}$$

where Eq. (10a) gives the Helmholtz energy in terms of the total partition function and Eq. (10b) in terms of Q_{int} and Q_{trans}. In the following equations, (a) and (b) have the same definition as in Eqs. (10a) and (10b).

The enthalpy is given by

$$H(T) = RT\frac{\tilde{Q}'}{Q} + RT \tag{11a}$$

$$H(T) = RT\frac{\tilde{Q}'_{\text{int}}}{Q_{\text{int}}} + \frac{7}{2}RT. \tag{11b}$$

JANAF[38] or Furtenbacher *et al.*[23] define a quantity called the standardized enthalpy given by

$$hef(T) = \overline{H}(T) - E_0 = RT\frac{\tilde{Q}'}{Q} - RT - H(298.15\ \text{K}) \tag{12a}$$

$$hef(T) = RT\frac{\tilde{Q}'_{\text{int}}}{Q_{\text{int}}} + \frac{5}{2}RT - H(298.15\ \text{K}), \tag{12b}$$

where E_0 is H at 298.15 K.

The entropy is given by $-\partial A/\partial T$

$$S(T,p) = R\left(T\frac{\mathrm{d}\ln Q}{\mathrm{d}T} + \ln Q\right) = R\left(\frac{\tilde{Q}'}{Q} + \ln Q\right) \tag{13a}$$

$$S(T,p) = R\frac{\tilde{Q}'_{\text{int}}}{Q_{\text{int}}} + R\ln Q_{\text{int}} + \frac{5}{2}R + R\ln\frac{(2\pi m)^{3/2}(kT)^{5/2}}{h^3 p}. \tag{13b}$$

The Gibbs energy is given by

$$G(T) = -RT \ln Q + RT \tag{14a}$$

$$G(T) = -RT \ln Q_{\text{int}} - RT \ln\frac{(2\pi m)^{3/2}(kT)^{5/2}}{h^3 p} + RT. \tag{14b}$$

JANAF,[38] Gurvich,[39] and others[23,34,40] define the Gibbs energy function

$$gef(T) = -\frac{[G(T) - E_0]}{T} = R \ln Q + \frac{H(298.15\ \text{K})}{T} \tag{15a}$$

$$gef(T) = R \ln Q_{\text{int}} + R \ln\frac{(2\pi m)^{3/2}(kT)^{5/2}}{h^3 p} + \frac{H(298.15\ \text{K})}{T}, \tag{15b}$$

where E_0 was defined above.

Finally, the ideal gas isobaric heat capacity is

$$C_p = R\left[\frac{\tilde{Q}''}{Q} - \left(\frac{\tilde{Q}'}{Q}\right)^2\right] \tag{16a}$$

$$C_p(T) = R\left[\frac{\tilde{Q}''_{\text{int}}}{Q_{\text{int}}} - RT\left(\frac{\tilde{Q}'_{\text{int}}}{Q_{\text{int}}}\right)^2\right] + \frac{5}{2}R \tag{16b}$$

and the ideal gas isochoric heat capacity is $C_v = C_p - R$ or

$$C_v = R\left[\frac{\tilde{Q}''_{\text{int}}}{Q_{\text{int}}} - RT\left(\frac{\tilde{Q}'_{\text{int}}}{Q_{\text{int}}}\right)^2\right] + \frac{3}{2}R. \tag{17}$$

The isobaric heat capacity can also be written as $C_p(T) = \partial H/\partial T$, which yields the same formula as Eq. (16). The thermodynamic functions were determined using both the total partition sums and using the TIPS and the translational partition sums and the results agree.

As stated above, the convention in the JANAF and Gurvich *et al.* data sets is not to include the spin-independent nuclear factors. They do include the *e* and *f* splitting of the states. Thus when

comparing the results of this work for certain functions, a factor of $R\ln(1.5)$ must be added to the JANAF or Gurvich *et al.* data. For thermodynamic functions where there are ratios of Q and its moments (e.g., H, *hef*, C_p, C_v), no factor is needed and for functions that contain $\ln(Q_{\rm int})$ (A, S, G, *gef*), the factor of $R\ln(1.5)$ must be added.

Using the $Q_{\rm int}(T)$, $\tilde{Q}'_{\rm int}(T)$, and $\tilde{Q}''_{\rm int}(T)$ functions determined in Sec. 2.3, the thermodynamic quantities given by Eqs. (10b), (11b), (12b), (13b), (14b), (15b), and (16b) were evaluated at temperatures from 1 to 9000 K at 1 K intervals for each isotopologue. Note, at 298 K the grid point was changed to the reference temperature, 298.15 K.

3.1. Uncertainties in the thermodynamic functions

The $Q_{\rm int}(T)$, $Q'_{\rm int}(T)$, and $Q''_{\rm int}(T)$ functions and the $\tilde{Q}_{\rm int}(T)$, $\tilde{Q}'_{\rm int}(T)$, and $\tilde{Q}''_{\rm int}(T)$ determined in Sec. 2.3 were taken and the thermodynamic quantities given by Eqs. (10b), (11b), (12b), (13b), (14b), (15b), and (16b) and the uncertainty in the thermodynamic functions were determined for temperatures from 1 to 9000 K at 1 K intervals. As before, the uncertainty determination considered the uncertainty due to convergence and the uncertainty from the term values. The uncertainty for each thermodynamic function is reported at each temperature in the accompanying supplementary material.

3.2. Thermodynamic functions for a natural sample of NO gas

A natural sample of nitric oxide will contain six isotopologues in a ratio set by the natural isotopic abundance. Berglund and Wieser[41] report the isotopic abundances as 0.996 337 (^{14}N), 0.003 663 (^{15}N), 0.997 620 6 (^{16}O), 0.000 379 0 (^{17}O), and 0.002 000 4 (^{18}O) from which natural abundance of the isotopologues can be determined: 0.993 966 (^{14}N^{16}O), $0.365\,428 \times 10^{-2}$ (^{15}N^{16}O), $0.199\,307 \times 10^{-2}$(^{14}N^{18}O), $0.377\,612 \times 10^{-3}$(^{14}N^{17}O), $0.732\,747 \times 10^{-5}$(^{15}N^{18}O), and $0.138\,828 \times 10^{-5}$(^{15}N^{17}O). The thermodynamic functions (TF) for the natural sample can be calculated from those of the isotopologues,

$$\begin{aligned} TF(\text{natural sample}) = {} & 0.993\,966\ TF(^{14}\text{N}^{16}\text{O}) \\ & + 0.365\,428 \times 10^{-2} TF(^{15}\text{N}^{16}\text{O}) \\ & + 0.199\,307 \times 10^{-2} TF(^{14}\text{N}^{18}\text{O}) \\ & + 0.377\,612 \times 10^{-3} TF(^{14}\text{N}^{17}\text{O}) \\ & + 0.732\,747 \times 10^{-5} TF(^{15}\text{N}^{18}\text{O}) \\ & + 0.138\,828 \times 10^{-5} TF(^{15}\text{N}^{17}\text{O}) \end{aligned} \quad (18)$$

The uncertainty in the partition sums and its moments for the three lesser isotopologues is discussed above. For the three lesser isotopologues, the uncertainties in $Q_{\rm int}(T)$, $Q'_{\rm int}(T)$, and $Q''_{\rm int}(T)$ are respectively 0.10%, 0.25%, and 0.49% for ^{14}N^{17}O; 0.14%, 0.36%, and 0.73% for ^{15}N^{18}O; and 0.12%, 0.31%, and 0.63% for ^{15}N^{17}O. Note that the entropy of isotope mixing has been ignored on the grounds that it cancels in chemical reactions.

The JANAF data[38] and Gurvich *et al.*[39] data are for natural samples, however, in both cases it appears the calculations were done for the principal isotopologue. As mentioned above, because both data sets do not include the state-independent spin factors, for some thermodynamic functions a factor of $R\ln(1.5)$ must be added to the JANAF or Gurvich *et al.* values. Below, the differences that are observed are due to the formulations used by JANAF or Gurvich *et al.* to compute the energies. JANAF only considers the electronic ground $^2\Pi$ state with a degeneracy factor of 2, and Gurvich *et al.* consider the four lowest electronic states. Both use effective Hamiltonian formulations to determine energy levels.

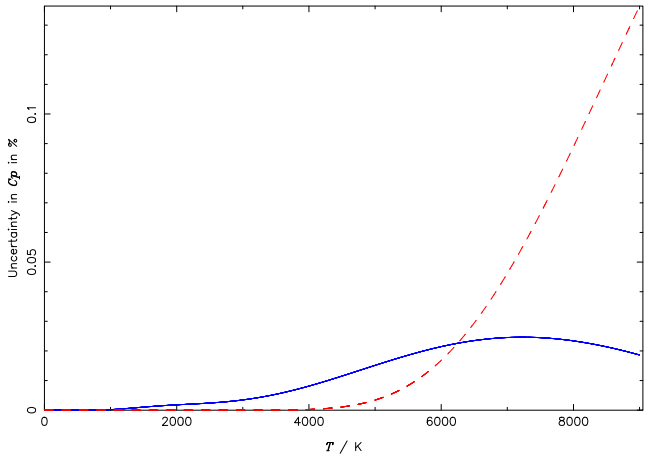

FIG. 4. The relative uncertainty in C_p from the uncertainty in the term values (blue solid line) and the uncertainty from convergence (red dashed line) versus temperature.

3.3. Isobaric heat capacity

The isobaric heat capacity, C_p, was determined using Eq. (16b). C_p is also given by $\partial H/\partial T$; both formulas were used as a check and the results agree. Figure 4 shows the uncertainty in C_p from the uncertainty in the term values and the error from convergence versus temperature. The uncertainty is near zero up to ~4000 K, after which the uncertainty from the term values reaches ~0.019% and that from convergence reaches ~0.135% at 9000 K.

Figure 5 shows C_p data (J mol^{-1} K^{-1}) for a natural sample from this work, JANAF data[38] and Gurvich *et al.*[39] versus temperature. Small differences are seen below ~4000 K. The JANAF data reaches about 0.5% at 4200 K and then increases to roughly 1.3% at 6000 K. The Gurvich *et al.* values reach roughly −0.5% at ~5350 K and then go down to ~−13% at 9000 K. Some examples of the data are presented in Table 1; the full table is presented in the supplementary material. Both tables include the C_p data computed using the NASA polynomial of Wang *et al.*,[1] which is for ^{14}N^{16}O. Note that the NASA polynomials are generally applied from 200–6000 K; for ^{14}N^{16}O the maximum temperature reported is 5000 K.

3.4. Entropy

The entropy, S^0, was calculated via Eq. (13b) and the uncertainty analysis done. The uncertainty from the term values reaches ~2.2×10^{-3}% and the uncertainty from convergence reaches ~5.6×10^{-2}% (see Fig. 5S for details). Figure 6 shows the PD between the entropy calculated via Eq. (13b) for a natural sample and that

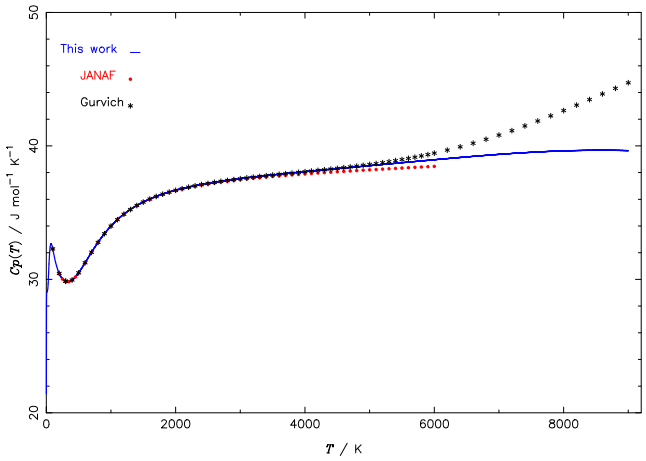

FIG. 5. C_p data from this work for a natural sample (blue line), JANAF data (red solid circles), and Gurvich *et al.* (black asterisks) versus temperature.

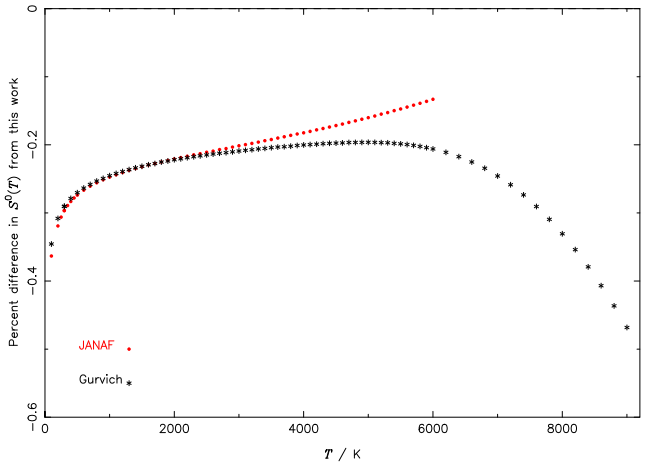

FIG. 6. The percent difference between the entropy calculated via Eq. (13b), S^0 for a natural sample and that from the JANAF data + $R\ln(1.5)$ (red solid circles) and from Gurvich *et al.* + $R\ln(1.5)$ (black asterisks) versus temperature.

TABLE 1. Partial table of isobaric heat capacity for a natural sample of NO from this work, Gurvich *et al.*,[39] JANAF,[38] and Wang *et al.* ($^{14}N^{16}O$)[1] in units of J mol^{-1} K^{-1}

T (K)	C_p this work	C_p Gurvich *et al.*	C_p JANAF	C_p Wang *et al.*
1.00	21.4217			
10.00	29.0644			
100.00	32.2821	32.283	32.302	
200.00	30.4445	30.445	30.420	30.4338
250.00	30.0459		30.025	30.0482
298.15	29.8618	29.862	29.845	29.8572
300.00	29.8580	29.858	29.841	29.8532
350.00	29.8365		29.823	29.8331
500.00	30.4944	30.493	30.486	30.4888
800.00	32.7729	32.770	32.767	32.7443
1000.00	33.9936	33.990	33.987	33.9331
2000.00	36.6800	36.673	36.647	36.6801
3000.00	37.5518	37.540	37.466	37.5501
4000.00	38.0718	38.063	37.898	38.0683
5000.00	38.5196	38.606	38.208	38.5123
6000.00	38.9638	39.454	38.468	

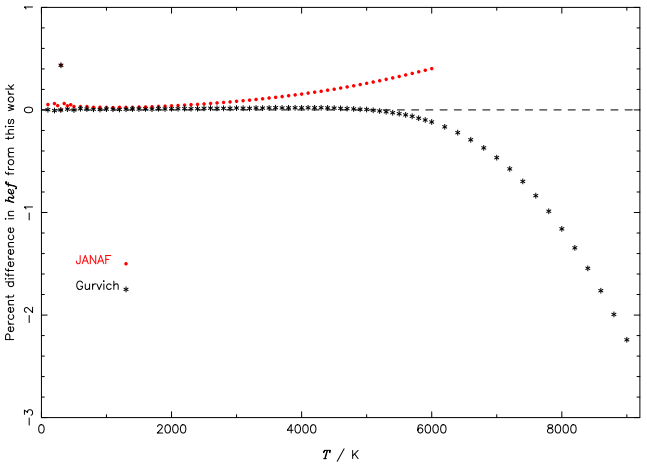

FIG. 7. The percent difference in the enthalpy function, *hef*, from this work, Eq. (12b) for a natural sample, and that from the JANAF data (red solid circles) and from Gurvich *et al.* (black asterisks) versus temperature.

from the JANAF data[38] + $R\ln(1.5)$ (red solid circles) and from Gurvich *et al.*[39] + $R\ln(1.5)$ (black asterisks) versus temperature. The PDs range between ~−0.36 at 100 K and ~−0.5 at 9000 K. These values of S at 298.15 K in J mol^{-1} K^{-1} are: this work 213.506 01 ± 0.000 00, JANAF + $R\ln(1.5)$ 214.129 23, Gurvich *et al.* + $R\ln(1.5)$ 214.116 23.

3.5. Enthalpy function

The enthalpy function was calculated via Eq. (12b) and the uncertainty due to convergence of the partition sum and its moments and that due to the uncertainty in the term values was determined. The uncertainties at 9000 K reach 0.010% and 0.017% for the uncertainty from term values and the uncertainty from convergence (see Fig. 6S for details). Figure 7 shows the PD in the enthalpy function, *hef*, for a natural sample from this work, Eq. (12b) and that from the JANAF data and from Gurvich *et al.* versus temperature. The JANAF data reach ~0.36% at 6000 K and the Gurvich *et al.* data reach ~−2.28% at 9000 K.

3.6. Gibbs energy function

The Gibbs energy function, *gef*, was determined using Eq. (15b). The uncertainty in the calculated *gef* is slightly larger for the term values up to roughly 5000 K and then dominated by the uncertainty due to the convergence. The maximum uncertainty values are 8.3 × 10^{-4}% for the term values and 4.5 × 10^{-4}% for the convergence (see Fig. 7S for details). Gurvich *et al.*[39] define $\Phi = -G/T$ thus, *gef* is given by $[\Phi T + H(T_{\mathrm{ref}})]/T$. The Gibbs

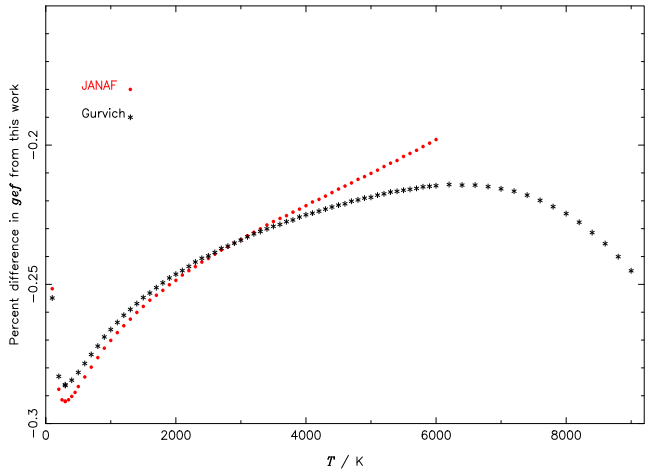

FIG. 8. The percent difference in Gibbs energy function, *gef*, determined here compared with that from JANAF + $R\ln(1.5)$ (red solid circles) and Gurvich *et al.* + $R\ln(1.5)$ (black asterisks) versus temperature.

energy function, *gef*, determined here is compared with that from the JANAF data + $R\ln(1.5)$ and that of Gurvich *et al.* + $R\ln(1.5)$ in Fig. 8. Shown is the PD between the *gef* from this work and that from the JANAF tables + $R\ln(1.5)$ (red solid circles) and that from Gurvich *et al.* + $R\ln(1.5)$ (black asterisks). The PD ranges from ~−0.2 to −0.3.

4. Conclusions

The ideal gas total partition sum and its first and second moments, $Q(T)$, $\tilde{Q}'(T)$, and $\tilde{Q}''(T)$, were determined via the TIPS and the translational partition sum. The TIPS and its moments were determined using very accurate sets of term values of Qu *et al.*[30] for the rovibronic $X^2\Pi$, $A^2\Sigma^+$, $B^2\Pi$, and $C^2\Pi$ states of $^{14}N^{16}O$ and Wong *et al.*[29] for the rovibronic $X^2\Pi$ states of $^{15}N^{16}O$, $^{14}N^{18}O$, $^{14}N^{17}O$, $^{15}N^{18}O$, and $^{15}N^{17}O$. Using the partition sums and moments, the following thermodynamic functions were determined from 1 to 9000 K: the Helmholtz function (A), the enthalpy (H), the entropy (S), the Gibbs energy (G), the isobaric heat capacity (C_p), and the JANAF functions: the standardized enthalpy (*hef*), and the Gibbs energy function (*gef*). The uncertainty in all quantities is taken as the uncertainty from the term values plus the uncertainty from the convergence of $Q_{int}(T)$, $Q'_{int}(T)$, and $Q''_{int}(T)$ and were determined as a function of temperature. Finally, tables were made for all quantities giving the final values over the temperature range from 1 to 9000 K in 1 K steps, with the exception that at 298 K data are given for 298.15 K, the reference temperature. Provided in the supplementary material are the figures mentioned in the text, a table of C_p data from this work, and the work of JANAF,[38] Gurvich *et al.*,[39] and Wang *et al.*[1] For the three most abundant isotopologues: a table of the TIPS and its first and second moments and the uncertainty in each quantity from 1 to 9000 K, and a table of the thermodynamic functions, including a table for the natural sample: $C_p(T)$, $A(T)$, $S(T)$, *hef*(T), *gef*(T), $H(T)$, and $G(T)$, each with uncertainty, from 1 to 9000 K. $C_p(T)$, $S(T)$, and *gef*(T) are in units of J mol^{-1} K^{-1} and $A(T)$, *hef*(T), $H(T)$, and $G(T)$ are in units of J mol^{-1}. It is noted that the $^{14}N^{16}O$ term values used in these calculations go above the dissociation limit[35] (i.e., include metastable states). It should be realized that at elevated temperatures the system is probably no longer in Local-Thermodynamic Equilibrium (LTE) and non-LTE corrections should be made.[42]

5. Supplementary Material

Provided in the supplemental data are the figures mentioned in the text, a table of C_p data from this work, and the work of JANAF,[38] Gurvich *et al.*,[39] and Wang *et al.*[1] For the three most abundant isotopologues: a table of the TIPS and its first and second moments and the uncertainty in each quantity from 1 to 9000 K, and a table of the thermodynamic functions including a table for the natural sample: $C_p(T)$, $A(T)$, $S(T)$, *hef*(T), *gef*(T), $H(T)$, and $G(T)$, each with uncertainty, from 1 to 9000 K. $C_p(T)$, $S(T)$, and *gef*(T) are in units of J mol^{-1} K^{-1} and $A(T)$, *hef*(T), $H(T)$, and $G(T)$ are in units of J mol^{-1}.

File 1. Complete version of Table I; isobaric heat capacity for a natural sample from this work, Gurvich *et al.*,[39] JANAF,[38] and Wang *et al.* ($^{14}N^{16}O$)[1] in units of J mol^{-1} K^{-1}.

File 2. Table of the TIPS and its first and second moments and the uncertainty in each quantity for $^{14}N^{16}O$. (NO_46_final_QofT_w_uncertainty_2024.txt).

File 3. Table of the thermodynamic functions for $^{14}N^{16}O$: $C_p(T)$, $A(T)$, $S(T)$, *hef*(T), *gef*(T), $H(T)$, and $G(T)$ each with uncertainty from 1 to 9000 K. $C_p(T)$, $S(T)$, and *gef*(T) are in units of J mol^{-1} K^{-1} and $A(T)$, *hef*(T), $H(T)$, and $G(T)$ are in units of J mol^{-1}. (NO_46_final_functions_w_uncertainty_2024.txt).

File 4. Table of the TIPS and its first and second moments and the uncertainty in each quantity for $^{15}N^{16}O$. (NO_56_final_QofT_w_uncertainty_2024.txt).

File 5. Table of the thermodynamic functions for $^{15}N^{16}O$: $C_p(T)$, $A(T)$, $S(T)$, *hef*(T), *gef*(T), $H(T)$, and $G(T)$ each with uncertainty from 1 to 9000 K. $C_p(T)$, $S(T)$, and *gef*(T) are in units of J mol^{-1} K^{-1} and $A(T)$, *hef*(T), $H(T)$, and $G(T)$ are in units of J mol^{-1}. (NO_56_final_functions_w_uncertainty_2024.txt).

File 6. Table of the TIPS and its first and second moments and the uncertainty in each quantity for $^{14}N^{18}O$. (NO_48_final_QofT_w_uncertainty_2024.txt).

File 7. Table of the thermodynamic functions for $^{14}N^{18}O$: $C_p(T)$, $A(T)$, $S(T)$, *hef*(T), *gef*(T), $H(T)$, and $G(T)$ each with uncertainty from 1 to 9000 K. $C_p(T)$, $S(T)$, and *gef*(T) are in units of J mol^{-1} K^{-1} and $A(T)$, *hef*(T), $H(T)$, and $G(T)$ are in units of J mol^{-1}. (NO_48_final_functions_w_uncertainty_2024.txt).

File 8. Table of the thermodynamic functions for a natural sample of NO gas: $C_p(T)$, $A(T)$, $S(T)$, *hef*(T), *gef*(T), $H(T)$, and $G(T)$ each with uncertainty from 1 to 9000 K. $C_p(T)$, $S(T)$, and *gef*(T) are in units of J mol^{-1} K^{-1} and $A(T)$, *hef*(T), $H(T)$, and $G(T)$ are in units of J mol^{-1}. (NO_NS_final_functions_w_uncertainty_2024.txt).

File 9. Derivation of the thermodynamic quantities in terms of the partition sum and its first and second derivatives and the partition sum and its first and second moments.

File 10. The supplementary figures (1S–7S) mentioned in the text.

6. Author Declarations

6.1. Conflict of interest

The authors have no conflicts to disclose.

7. Data Availability

The data that support the findings of this study are available within the article and its supplementary material and are openly available on zenodo at https://doi.org/10.5281/zenodo.12635229.

8. References

[1] R. Wang, U. Balciunaite, J. Chen *et al.*, J. Quant. Spectrosc. Radiat. Transfer **306**, 108617 (2023).
[2] D. McGongle, L. M. Ziurys, W. M. Irvine *et al.*, Astrophys. J. **359**, 121–124 (1990).
[3] M. Gerin, Y. Viala, F. Pauzat *et al.*, Astron. Astrophys. **266**, 463–478 (1992).
[4] M. Gerin, Y. Viala, and F. Casoli, Astron. Astrophys. **268**, 212–214 (1993).
[5] S. Martín, R. Mauersberger, J. Martín-Pintado *et al.*, Astron. Astrophys. **411**, L465–L468 (2003).
[6] S. Martín, R. Mauersberger, J. Martín-Pintado *et al.*, "The dense interstellar medium in galaxies," in *4th Cologne-Bonn-Zermatt-Symposium* (Springer, 2003), pp. 22–26.
[7] S. Martín, R. Mauersberger, J. Martín-Pintado *et al.*, Astrophys. J., Suppl. Ser. **164**, 450 (2006).
[8] M. Akyilmaz, D. R. Flower, P. Hily-Blant *et al.*, Astron. Astrophys. **462**, 221–230 (2007).
[9] G. Quintana-Lacaci, M. Agúndez, J. Cernicharo *et al.*, Astron. Astrophys. **560**, L2 (2013).
[10] G. N. Tsurikov and D. V. Bisikalo, Astron. Rep. **67**, 1123–1138 (2023).
[11] R. W. Eastes, R. E. Huffman, and F. J. Leblanc, Planet. Space Sci. **40**, 481–493 (1992).
[12] J.-C. Gérard, C. Cox, A. Saglam *et al.*, J. Geophys. Res.: Planets **113**, E00B03 (2008).
[13] C. Cox, A. Saglam, J.-C. Gérard *et al.*, J. Geophys. Res.: Planets **113**, E08012 (2008).
[14] I. E. Gordon, L. S. Rothman, R. J. Hargreaves *et al.*, J. Quant. Spectrosc. Radiat. Transfer **277**, 107949 (2022).
[15] R. C. Flagan and J. H. Seinfeld, *Fundamentals of Air Pollution Engineering* (Prentice-Hall, Englewood Cliffs, NJ, 1988).
[16] R. G. Barry and R. J. Chorley, *Atmosphere, Weather and Climate* (Van Nostrand Reinhold, London; New York, 2010).
[17] R. P. Wayne, *Chemistry of Atmospheres* (Oxford University Press, Oxford, 2000).
[18] T. Delahaye, R. Armante, N. A. Scott *et al.*, J. Mol. Spectrosc. **380**, 111510 (2021).
[19] A. J. Sauval and J. B. Tatum, Astrophys. J., Suppl. Ser. **56**, 193–209 (1984).
[20] E. Tiesinga, P. J. Mohr, D. B. Newell, and B. N. Taylor, J. Phys. Chem. Ref. Data **50**, 033105 (2021).
[21] R. R. Gamache, C. Roller, E. Lopes *et al.*, J. Quant. Spectrosc. Radiat. Transfer **203**, 70–87 (2017).
[22] R. R. Gamache, B. Vispoel, M. Rey *et al.*, J. Quant. Spectrosc. Radiat. Transfer **271**, 107713 (2021).
[23] T. Furtenbacher, T. Szidarovszky, J. Hrubý *et al.*, J. Phys. Chem. Ref. Data **45**, 043104 (2016).
[24] G. Herzberg, *Molecular Spectra and Molecular Structure I. Spectra of Diatomic Molecules* (D. Van Nostrand Company, NJ, 1950).
[25] R. R. Gamache, S. Kennedy, R. Hawkins, and L. S. Rothman, J. Mol. Struct. **517–518**, 407–425 (2000).
[26] G. Herzberg, *Molecular Spectra and Molecular Structure II. Infrared and Raman Spectra of Polyatomic Molecules* (D. Van Nostrand Company, NJ, 1960).
[27] W. L. Meerts, Chem. Phys. **14**, 421–425 (1976).
[28] C. Amiot, R. Bacis, and G. Guelachvili, Can. J. Phys. **56**, 251–265 (1978).
[29] A. Wong, S. N. Yurchenko, P. Bernath *et al.*, Mon. Not. R. Astron. Soc. **470**, 882–897 (2017).
[30] Q. Qu, S. N. Yurchenko, and J. Tennyson, Mon. Not. R. Astron. Soc. **504**, 5768–5777 (2021).
[31] T. Furtenbacher, M. Horváth, D. Koller *et al.*, J. Phys. Chem. Ref. Data **48**, 023101 (2019).
[32] R. R. Gamache and N. G. Orphanos, J. Phys. Chem. Ref. Data **52**, 023101 (2023).
[33] J. M. L. Martin, J. P. François, and R. Gijbels, J. Chem. Phys. **96**, 7633–7645 (1992).
[34] M. Vidler and J. Tennyson, J. Chem. Phys. **113**, 9766–9771 (2000).
[35] A. B. Callear and M. J. Pilling, Trans. Faraday Soc. **66**, 1618–1634 (1970).
[36] T. Furtenbacher, A. G. Császár, and J. Tennyson, J. Mol. Spectrosc. **245**, 115–125 (2007).
[37] T. Furtenbacher and A. G. Császár, J. Quant. Spectrosc. Radiat. Transfer **113**, 929–935 (2012).
[38] M. W. Chase, Jr., C. A. Davies, J. R. Downey *et al.*, J. Phys. Chem. Ref. Data **14**(Suppl. 1), 1–1856 (1985).
[39] L. Gurvich, I. V. Veyts, C. B. Alcock *et al.*, *Thermodynamic Properties of Individual Substances: Elements and Compounds*, 4th ed. (Hemisphere, New York, 1991).
[40] B. Ruscic, J. Phys. Chem. A **117**, 11940–11953 (2013).
[41] M. Berglund and M. E. Wieser, Pure Appl. Chem. **83**, 397–410 (2011).
[42] R. R. Gamache, B. Vispoel, M. Rey *et al.*, Icarus **378**, 114947 (2022).